

DI 206259

# waterloopkundig laboratorium delft hydraulics laboratory

een eenvoudig rekenschema voor de berekening  
van toegevoegde watermassa bij schuiven

presentatie rekenprogramma

Q 491

november 1987

C 12418

C 51

**tow**

toegepast onderzoek  
waterstaat

---

een eenvoudig rekenschema voor de berekening  
van toegevoegde watermassa bij schuiven

presentatie rekenprogramma

---

Q 491

november 1987

C 51

**tow**

toegepast onderzoek  
waterstaat

## INHOUD

	blz.
1. Inleiding.....	2
2. Samenvatting van de resultaten.....	2

Bijlage 1 Paper in te dienen in Journal of Fluids and Structures,  
"A simple scheme for calculating the added mass of gates"

Bijlage 2 Het rekenprogramma en voorbeeld berekening waarbij een verticale  
klep op een vlakke bodem staat en een roterende trilling uitvoert



## 1. Inleiding

In 1984 is in het kader van een speurwerkprogramma van de TU in Delft een rekenprogramma ontwikkeld voor het bepalen van de toegevoegde watermassa bij schuiven en kleppen. In [1] zijn de formules en de randvoorwaarden afgeleid, en is het rekenprogramma getoetst.

Toegevoegde watermassa berekeningen zijn van belang bij het berekenen van krachten bij het versnellen en afremmen van punt- en klepdeuren van schutsluizen, bij trillingsberekeningen aan schuiven die door omstroming of lekstroming potentieel kunnen gaan trillen en bij golfbelasting op constructies.

De berekening die met een kort rekenprogramma is uit te voeren (zie bijlage 2) kan op een PC worden uitgevoerd. Een variant hiervan is het gebruik van een spread-sheet programma.

De spread-sheet methode heeft als voordeel het snel en eenvoudig programmeren, ook als de schuifpositie en waterstanden een aantal malen moet variëren. De programma-wijzigingen vergen geen programma ervaring. Nadeel van het spread-sheet is dat het rekenen zeer langzaam gaat.

In het kader van TOW-kunstwerken is een IBM-P.C. variant ontwikkeld waarbij het programmeren wel enige ervaring vereist, maar wijzigen van de randvoorwaarden kan ook nu snel gebeuren, terwijl de rekentijd veel korter is. In deze nota wordt het programma met een korte toelichting gepresenteerd terwijl in bijlage 1 een artikel (nog niet ingediend) is bijgevoegd waarin de gebruikte formules zijn afgeleid, waarin tests staan betreffende de te bereiken nauwkeurigheid, en waarin voor een paar gevallen rekenresultaten staan vermeld. Het betreft hier berekeningen aan kleppen die op een vlakke vloer of op een drempel staan.

De opstelling van de PC-versie, de berekeningen en de rapportering zijn gedaan door Dr. Ir. P.A. Kolkman en hebben plaats gevonden in de periode september tot november 1987. De IBM-versie (in Fortran) is opgesteld door ir. J. van Huystee.

## 2. Samenvatting van de resultaten

Zoals uit bijlage 1 volgt is het rekenprogramma getoetst. Afhankelijk van hoe groot het aantal elementen is waarin de schuif is verdeeld, is een nauwkeurigheid van een paar procent te bereiken. Er is in bijlage 1 een schatting te vinden van het aantal berekeningen en aantal iteraties dat nodig is om redelijk nauwkeurig de limietwaarde te bereiken. Tevens is een automatisch werkend stopkriterium ingevoerd om de berekening te stoppen. De nauwkeurigheid van de rekenresultaten is het grootst voor translaterende schuiven waarbij de rand niet omstroomt (dus als de schuif boven water uit steekt). De nauwkeurigheid is het kleinst bij roterende kleppen met omstroming (zelfs bij 10 elementen is er nog 15% afwijking).

De procedure die gevolgd is, is steeds geweest dat eerst een aantal berekeningen is uitgevoerd met een grof rooster (korte rekentijd) om de horizontale en vertikale uitgestrektheid te toetsen, en daarna wordt de berekening herhaald met een veel fijner rooster waarbij de PC bijvoorbeeld een nacht kan doorrekenen. Een twee maal fijner rooster betekent viermaal meer roosterpunten en een bijna viermaal groter aantal iteraties, dus 16x meer rekentijd.

Gedetailleerde conclusies en rekenresultaten voor translaterende en roterende kleppen zijn in bijlage 1 te vinden.

Het programma in bijlage 2 is voorzien van een aantal opmerkingen als toelichting zodat het voor de lezer eenvoudig is het naar bevind van zaken te wijzigen afhankelijk van de schuif en drempelgeometrie en afhankelijk of het schuiftranslatie of rotatie betreft.

### Literatuur

- 1 Kolkman, P.A.; "Opzet eenvoudig 2-dimensionaal rekenprogramma ter bepaling van de toegevoegde watermassa" Notities 1 en 2 uit de serie "Hydrodynamische massa", TH Delft, afd. CT vakgroep Waterbouw Sept-Dec '84



A Simple Scheme for Calculating  
the Added Mass of Gates

by:

P.A. Kolkman  
Senior Expert DELFT HYDRAULICS,  
Dept. of Rivers, Navigation and Structures, and  
Senior Research Officer Technical University Delft,  
Dept. Civil Engineering

Summary

In gate research and design, added mass calculation serves to establish resonance frequencies, vibration modes and the magnitude of flow-induced self-excitation and damping. The fluid boundary geometries vary strongly with gate position and water level variation.

A relatively simple and versatile computation scheme is presented which is based on two dimensional potential flow without wave radiation. Only small amplitude vibrations are considered. A square mesh grid is used and the potential flow problem is solved by use of finite differences and the classical pointwise Gauss-Seidel iteration (relaxation) method. When the spread sheet type calculation is used boundary conditions and boundary locations can easily be varied; this makes it suitable for demonstration purpose.

Presented are the boundary conditions, and how they are introduced in the computation scheme. The accuracy of the results is discussed for some cases for which analytical solutions exist: the vibrating strip and the vibrating wall. The number of relaxations needed, the use of overrelaxation and the introduction of an automatic stop of the calculation are other elements of the paper.

Running headline: Added-Mass of gates

## 1. Introduction

Knowledge concerning the added mass of a body which is totally or partly submerged in liquid is needed for the calculation of:

- Resonance frequencies of structures,
- Coupling effects induced by the added mass and resulting in modification of the vibration mode or in coupled vibrations when several bodies are involved,
- Wave forces (Morisson concept),
- Wave shock and slamming pressures,
- Earthquake loads on dams,
- Self-excitation magnitudes of vibrating gates.

It is the author's experience that especially in gate research one has to deal with a number of problems where added mass calculations are needed in which a great number of geometries are involved. Even in designing one gate, the gate position and water level are variables. The calculation may usually be reduced to a two-dimensional problem.

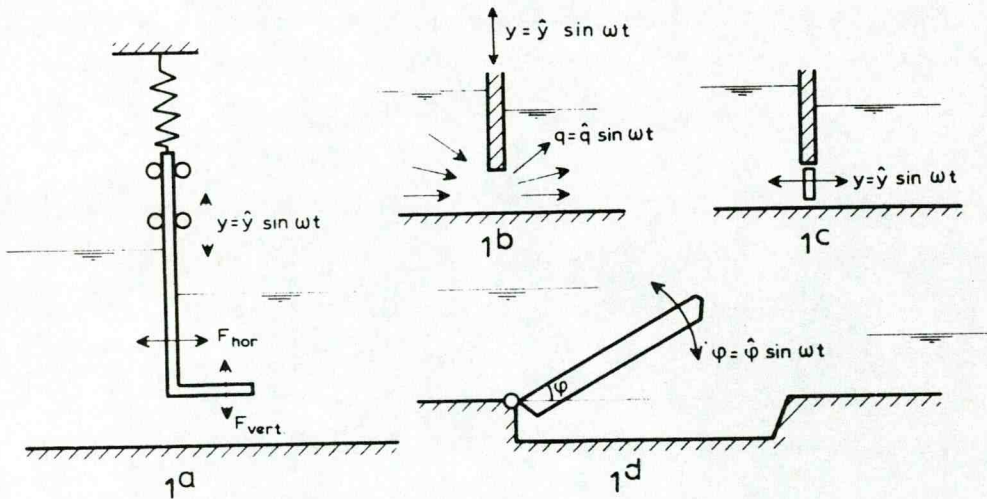


Figure 1. Various geometries involved in gate vibrations problems.

Represented in Figure 1 are:

- 1a The coupling forces induced by the added mass where vertical acceleration gives a horizontal force component and vice versa. In fact, each vibrating boundary element induces pressures at all the other boundary elements. The concept of added-mass matrix is found, among others, in Jennings [2] and Kolkman [4].



- 1b A gate vibrating vertically so that the flow is periodically throttled. The combination of discharge fluctuations and the inertia of the water up- and downstream of the gate results in periodic forces acting on the gate which can cause either damping or self-excitation, [3] and [4].
- 1c A valve placed low in a dam, experiences a similar added mass effect as caused by flow inertia in 1b.
- 1d A vibrating flap gate inducing boundary displacements which are proportional to their distance to the hinge; the added mass effect becomes an added polar moment of inertia.

Vibration calculations of gates are generally based on small amplitude assumptions. Because the aim of these calculations is to prevent vibrations, it is important to know whether there is a tendency for instability at small amplitudes. Therefore, the added mass and the waterdamping (which at self-excitation conditions appears to become negative) are calculated for small vibration amplitudes.

For gates wave radiation can be neglected, because at higher vibration frequencies the wave length of radiated waves is small compared to the gate dimensions and to the water depth. Even an extremely low 2 Hz frequency has a  $\lambda_{\text{wave}}$  of 0.4 m, which is small in relation to the size of sluice gates and other gates where free-surface flow occurs. An earlier analysis for a configuration as in Figure 1c, (see [3]) showed that, when for horizontally vibrating gates the value  $\omega^2 h/g$  ( $\omega$  = angular frequency,  $h$  = waterdepth) is above 20, neglecting of wave radiation results in a deviation of the added mass of less than 5% from the high-frequency limit value.

The author has shown before [3] that another factor is far more important than wave radiation for the water damping of vibrating gates, and this is the extra energy loss produced by the oscillating free flow passing over the gate or the flow through the gap under the gate. This extra energy loss is produced when the vibrating gate produces velocity fluctuations. These velocity fluctuations produce an extra head loss across the gap but they also produce extra pressures at the gate surface and their coupled effect can be calculated by using added mass calculations.

The calculation was performed for a horizontally vibrating gate using a configuration like Figure 1b. The calculation consisted of a superposition of three components: an added mass calculated under the assumption that flow



under the gate was zero (blocked), an added mass calculated for the condition wherein the gate did not vibrate but the flow under the gate varied periodically, and the periodically varying local head difference across the gate related (by the discharge equation) to the periodic flow variation. Each component included the use of a calculated added mass and coupling effect, neglecting wave radiation and even the influence of steady flow on the added masses. Although the assumptions which were introduced in the calculation seem to be crude, the results were quite satisfying when compared to experimental results.

When the cases of Figure 1 are considered, gate positions and water levels are variable, so geometries are manifold. On the other hand, great accuracy is not necessary; 5-20% inaccuracy is already a useful result, depending on its application and other inaccuracies involved.

The need was felt for the development of a versatile computer program that can be implemented on a personal computer, is easy to handle and wherein geometries can be quickly varied. The acceptable neglect of wave radiation and the limitation to calculations in two dimensions and for small-amplitude vibrations only, result in simplifications similar to those introduced in some of the former methods, for instance using electric analogy with Teledeltos paper.

Remark:

When added-mass calculations are executed for offshore structures and ships, simplified calculations without wave radiation are not only applied for high-frequency vibrations but also for extremely low-frequency vibrations. In this case the free surface can be replaced in the computations by a rigid boundary. The second type of approximation, however, is not applicable to gates, because in half-space conditions, when the gate is nearly closed, a rigid free surface together with a finite water depth will result in infinite added-mass values which have no physical significance.

There were several possibilities readily available for added-mass calculations. The finite-element procedure, however, was considered to be too cumbersome for the great number of configurations needed, and with the boundary-element procedure the thin-plated gate caused an extra problem in finding the appropriate boundary-element distribution.



Olsthoorn [6] has shown the applicability of a spread sheet program for a two-dimensional potential flow calculation based on a relaxation method formerly taught in applied mechanics, which was called the Hardy-Cross method and is more generally known as the Gauss-Seidel method [1]. Spread sheet programming on a PC can be done without much skill. It presents a matrix wherein each element can contain an equation into which data or equations from other elements can be introduced. When one imagines the matrix elements to be elements of a fluid, the elements contain the same equation if they relate to the inner field and they contain different equations if they relate to one of the boundaries. Corner points need still other equations. The reason why a spreadsheet program can so easily be programmed is that equations used at the flow boundaries or in the inner flow can for each element be copied from the first element wherein this equation occurs and so the only thing needed is a set of equations for each of the type of elements. Further advantages are that variations of water level and gate position can be easily varied, that no special programming skill is needed and that this program is well suited for demonstration and educational purposes. A disadvantage of the spread sheet program is that it works relatively slow, which means that for demonstration purposes the number of computations (related to the number of grid points) should be limited.

The author has not used the spread sheet program himself, but one of our technicians has tried it out successfully and for the moment it seems that the program has essentially replaced the electric analog procedure which was formerly used at Delft Hydraulics. The disadvantages of using a regular rectangular grid, the neglect of wave radiation and the practical limitations on the number of grid points were accepted. For special checks more sophisticated programs are available.

Before the program was applied to projects some research was done into its accuracy. To this and a faster working program based on the same numerical scheme was used. This research was necessary because the disadvantage of a rectangular grid is that flow around sharp corners is one of its critical points, and this occurs frequently in gates.

This paper deals mainly with the boundary conditions, their introduction into the computation scheme and the accuracy tests.



## 2. Development of the basic equations

Without discussing the details, the potential flow theory with neglect of wave radiation is used in the following for added mass calculation. (See also Lamb [5], Wendel [7] and many others) Special caution is necessary because potential flow theoretically exists only in still water conditions and in small vibratory displacements. (In fact one assumes fixed contours and water displacement is introduced as source points) Application of the potential flow theory without wave radiation results in movements of the water elements which are all in phase and coupled with the vibratory movement of the structure. The amplitudes of the movement depend on the location.

The great simplification of the potential flow calculation is that the dynamic equation can be left out as an explicit expression and that only the continuity equation has to be fulfilled.

The basic equations for potential flow are:

$$\partial\Phi/\partial\bar{s} = -\bar{V} \quad (\text{the bar denotes a vector}) \quad (1)$$

( $\Phi$  = potential,  $V$  = fluid velocity and  $\partial s$  = a streamline element)

The velocity vector can be separated in x and y directions:

$$\bar{V}_x = -\frac{\partial\Phi}{\partial x} \quad (1a)$$

$$\bar{V}_y = -\frac{\partial\Phi}{\partial y} \quad (1b)$$

And when an oscillatory flow field is introduced (see [5]) one obtains:

$$p = \rho\partial\Phi/\partial t + \text{constant} \quad (2)$$

This equation is again a simplification; because only small amplitude vibrations are considered, as mentioned before,  $V^2$  terms tend to disappear and are neglected.

The boundary conditions are defined as follows:

1. For non-vibrating walls or lines of symmetry in the flow field we have:

$$\bar{V}_n = -\frac{\partial\Phi}{\partial\bar{n}} = 0 \quad (3)$$

( $\underline{n}$  = vector perpendicular to the boundary)

If one can expect symmetry in the flow field, only half the flow field needs to be calculated. On the line of symmetry equation 3 is valid (see line I in Figure 2).

2. For vibrating wall the boundary conditions are:

$$\frac{\partial \Phi}{\partial \bar{n}} = - \bar{V}_{sn} \quad (4)$$

( $\bar{V}_{sn}$  = component of the structural vibration velocity normal to the wall)

3. For free surfaces or lines of antisymmetry in the flow field there is introduced

$$\Phi = 0 \quad (5)$$

This follows from free surface wave theory when one assumes that gravity can be neglected.

We introduce a grid with square elements. See for notations Figures 2 and 4. The basic approach of the calculation here is the Gauss-Seidel iteration method [1] wherein the points are consecutively relaxed using the local continuity equation. The vibrating strip is used for demonstration of the proposed computation scheme, because in this case the exact solution is known and accuracy can be checked.

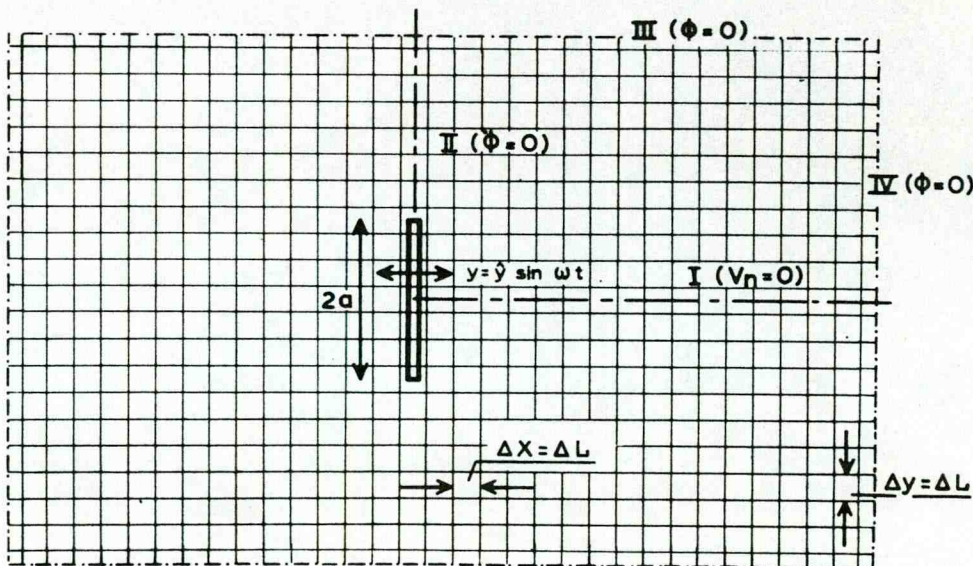


Figure 2. Representation of total grid wherein the sector enclosed by the boundaries I, II, III and IV is analysed.



The following elements of the computation are further considered: the significance of grid points, the chosen location of boundary elements, the boundary velocities (and resulting discharges) induced by the vibrating body, the resulting pressures and the definition of added mass.

- Each gridpoint represents an element of fluid with dimensions  $\Delta x$  and  $\Delta y$  and for simplicity there is chosen for  $\Delta x = \Delta y = \Delta L$ .
- The surfaces of the vibrating structure and of the other boundaries are schematized into elements of length  $\Delta L$  which are either horizontal or vertical. To obtain a homogeneous approach of the computations, the location of these boundary elements is chosen in between the grid points (see Figures 3 and 4).

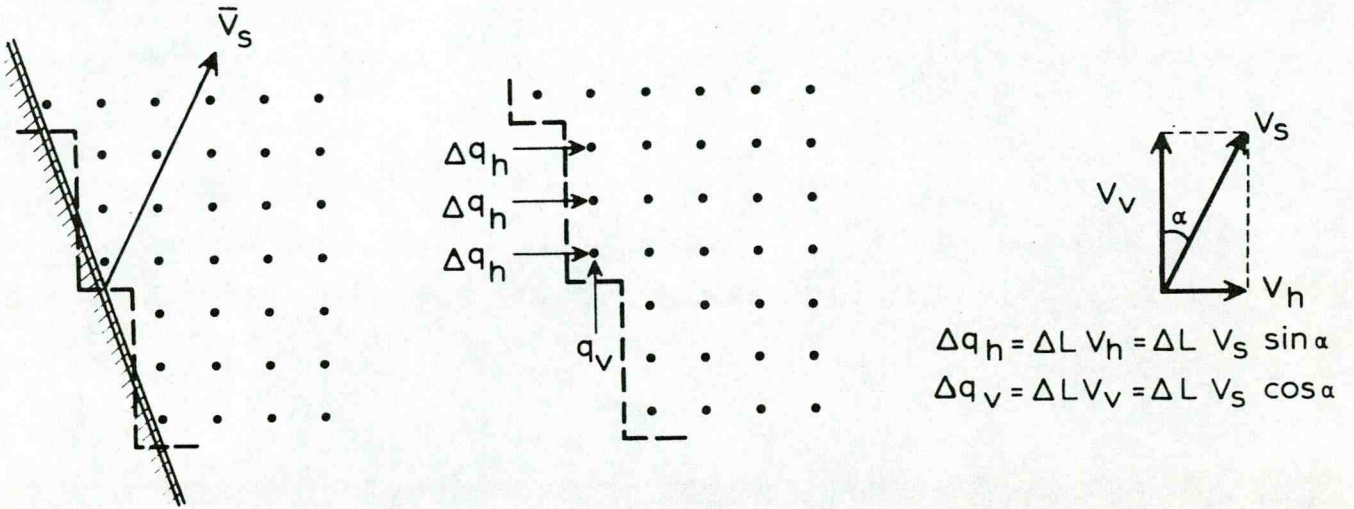


Figure 3. Boundary discharges at arbitrary angles to the boundary and to the vibration velocity.

- The definition of added mass of a vibrating structure is the vibration-induced hydrodynamic force component in the direction of vibration divided by the acceleration vector  $\bar{a}_s$ ,

$$m_w = \bar{F} / a_s \quad (6)$$

The force is determined by integration of the pressure influences along the boundary. So to start with, the acceleration vector of the (gate) boundaries is defined for either a translation or a rotation movement.

- A harmonic oscillation of the boundary is introduced in the form of a velocity vector  $\bar{V}_s = \hat{V}_s e^{i\omega t}$  and  $\bar{V}_s$  equals  $\bar{a}_s / i\omega$ .

- At an inclined wall of a vibrating gate the equivalent discharge produced by the velocity of a vertical element is (see Figure 3):

$$\Delta q_h = \bar{V}_h \Delta L = \bar{V}_s \Delta L \sin \alpha \quad (7a)$$

and for a horizontal element

$$\Delta q_v = \bar{V}_v \Delta L = \bar{V}_s \Delta L \cos \alpha \quad (7b)$$

- The potentials in the flow field are uniquely related to  $\bar{V}_s$  and the ratio  $(\phi/\bar{V}_s)$  is calculated with procedures presented in paragraphs 3 and 4. At the gate boundary we find the ratio  $(\phi_s/\bar{V}_s)$ .
- The dynamic part of the pressures  $p_s$  at the boundary are related by Equation 2, to the boundary potentials:

$$p_s = \rho \partial \phi_s / \partial t = \rho i \omega \phi_s \quad (8)$$

Because  $\phi_s$  is related to  $\bar{V}_s$ , which in turn equals  $\bar{a}_s/i\omega$ , the pressure  $\rho i \omega \phi$  is proportional to  $\rho \bar{a}_s$  (the proportionality is found by means of the ratio  $\phi_s/\bar{V}_s$ ). This proportionality means that the added mass is independent of  $\omega$  and that its use is not limited to periodic oscillations. This more general application for slamming calculations etc. is only adequate as long as gravity can be neglected.



### 3. Calculation of the potentials in the grid points

The calculation of the potential in each grid element uses only its continuity equation. The stream function is left out of consideration. At each point discharges arrive from four directions (index L refers to left, R to right, U to up, D to down) and hence

$$\Sigma \Delta q = \Delta q_L + \Delta q_U + \Delta q_R + \Delta q_D = 0 \quad (9)$$

When inner points are considered, the potential  $\phi$  at the point  $x, y$  (see Figure 4) can be calculated when we consider

$$\Delta q_L = V_L \Delta y = - \left. \frac{\partial \phi}{\partial x} \right|_L \Delta y \quad (10)$$

$V_L$  is the horizontal velocity at the left boundary of the element.

Because by approximation  $-\frac{\partial \phi}{\partial x} = -\Delta \phi / \Delta x = (\phi_L - \phi) / \Delta x$

and considering that  $\Delta x = \Delta y = \Delta L$ , one obtains

$$\Delta q_L = \phi_L - \phi \quad (11)$$

The distant boundaries (see Figure 2) are here represented by  $\phi = 0$ , but this is an arbitrary choice and  $V_n = 0$  would also have been possible. The determinant condition is that the boundary is far away. Now the calculation of the situation of Figure 2 can be restricted to one quadrant (symmetry and anti-symmetry lines are replaced by wall and free surface conditions). The resultant scheme is the one of Figure 4.

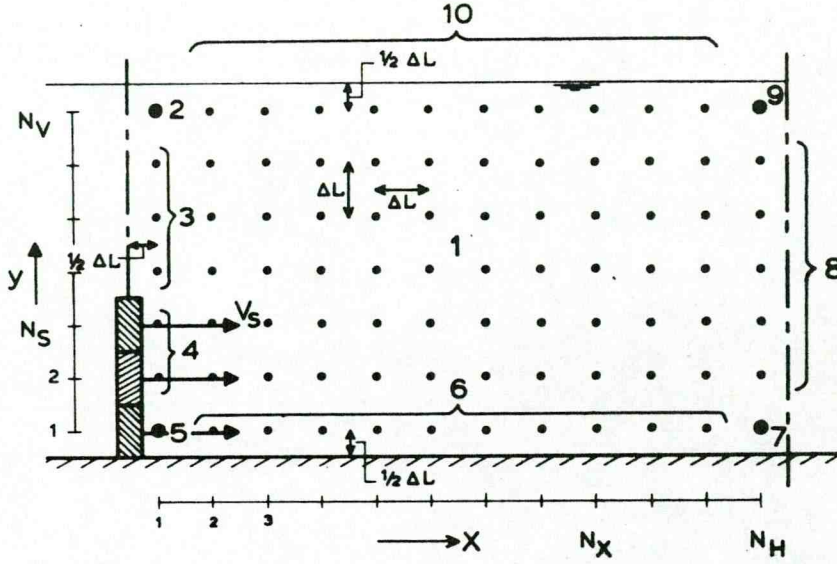


Figure 4. Definitions and localization of the elements.

When considering Figure 4, wherein the inner elements (represented by grid points) are indicated by 1, the upper left element by 2, etc., we find by combining equations 9 and 11:

1) for the inner elements

$$\Phi = (\Phi_L + \Phi_U + \Phi_R + \Phi_D)/4 \quad (12)$$

or

$$\Phi_{x,y} = (\Phi_{x-1,y} + \Phi_{x,y-1} + \Phi_{x+1,y} + \Phi_{x,y+1})/4 \quad (13)$$

(in the notations of Fig. 4, x should be read as  $N_x$  and y as  $N_y$ )

2) for the extreme upper left corner, with two boundaries for which  $\Phi = 0$  and each having a distance  $\frac{1}{2}\Delta L$  from the grid point (in the centre of the element), one gets for the discharge coming from the left side:

$$\Delta q_L = (\Phi_L - \Phi)/\frac{1}{2}$$



Because  $\phi_L = 0$ , this gives  $\Delta q_L = -2\phi$ .

The same is found for  $\Delta q_U$  and so, after application of the continuity equation 9, one finds:

$$\phi = (\phi_R + \phi_D)/6 \quad (14)$$

- 3) for the left elements above the gate no equation is worked out here; see appendix.
- 4) for the left elements at the right hand side of the gate (apart from the lowest one),  $\Delta q_L$  is directly derived from the gate movement, so

$$\phi = (\Delta q_L + \phi_U + \phi_R + \phi_D)/3 \quad (15)$$

The complete set of equations can be found in the appendix.

The boundary condition are in similar types of computation sometimes introduced by means of a set of virtual points outside the boundary. This method simplifies the calculations. It is not used here because thin-walled gates have real points at both sides of the boundary.

The solution used is the classical Gauss-Seidel iteration (relaxation). The sequence of relaxation can best be repetitively executed "away from the vibrating gate", and so in our case from left to right, until a limit of sufficient accuracy is reached. A stop criterium is introduced in Section 5; it can be introduced as an automatic stop or as a signal.

#### 4. Additional procedures

##### A. Overrelaxation

If the correction of the potential  $\phi$  during relaxation of a single point is greater than would follow from the equations derived in Section 3, the computation time can be considerably reduced. This procedure is known as SOR (successive overrelaxation, see [1]).

Taking only equation 12 as an example, and introducing an overrelaxation factor  $R$  (with  $R > 1$ ), we get

$$\phi_{\text{new}} = \phi_{\text{old}} + R(\phi - \phi_{\text{old}}) \quad (16)$$

So, equation 12 becomes

$$\phi_{\text{new}} = R(\phi_L + \phi_U + \phi_R + \phi_D)/4 + (1-R) \phi_{\text{old}} \quad (17)$$

Overrelaxation should not be too strong (say  $R = 1.5$  to  $1.7$ ), otherwise the process is not continuously convergent and overshoot or even divergence might occur. When overrelaxation is applied, it is desirable to print at regular intervals an output (for instance the average value of boundary potentials) to check whether such an overshoot has occurred.

##### B. Potentials at the boundaries of a vibrating body

When the potentials in points 4 and 5 in Figure 4 have been found, the potentials at the gate surface are obtained by

$$\phi_{\text{strip}} = \phi_{(4)\text{or}(5)} + \frac{1}{2}\Delta q_s \quad (18)$$

The term  $\frac{1}{2}\Delta q_s$  is the correction of the potential over a distance  $\frac{1}{2}\Delta L$  and equals  $\frac{1}{2}V_s \Delta L$  in the example of Figure 4.



5. The number of calculations. The introduction of a "Stop"-criterion

- A. By performing a calculation of extremely long duration, one could judge the number of times the whole grid has to be relaxed before a certain accuracy is reached. Without overrelaxation, it appeared that the number of relaxations needed for the configuration of Figure 4 was of the order of 0.5 to 0.7 times the number of grid points before an accuracy of 1% was reached.

With overrelaxation such a simple expression could not be found but the number of iterations was easily reduced by a factor four. So, at a first approximation, for a grid of dimensions  $N_H * N_V$  the total time of calculation becomes

$$\text{Time} = \Delta t (N_H * N_V)^2 0.7/4 \quad (19)$$

$\Delta t$  is the time needed for relaxation of one single point.

Because the number of grid points is squared, slow procedures like the spread sheet clearly have their limitations.

- B. There was a need, especially when using overrelaxation, to introduce an automatic criterion for stopping the calculation. This should be a non-dimensional criterion in the sense that it must be independant of the magnitude of the added mass obtained and of the number of iterations (the latter introduced as "time"  $t$ ). This is based on the fact that at the beginning of the calculations all the grid points start with a potential  $\phi = 0$ . When the added lengths (being the potentials at the boundary of the vibrating body) are now considered, a convergent solution is generally obtained (provided no instability results from too large an overrelaxation). Figure 5 shows the definition of the "Stop" criterion. The absolute value sign is introduced because too much overrelaxation sometimes gives an overshoot after which the derivative  $dF/dt$  remains negative. To get an idea whether such a stop criterion is generally applicable, it has been applied to three known analytical functions which converge to a limit value. These functions are

$$Y = \tanh t$$

$$Y = 1 - e^{-t}$$

$$Y = (2/\pi) \tan^{-1}(\pi t/2)$$

The result of the calculation experiments concerning the average added length versus these analytical functions is shown in Figure 6. It is apparent that the  $(\tan^{-1})$  function does not produce convergence as rapidly as the other two functions. The accuracy of the experiments is generally in accordance with or better than predicted by the two other functions. For all experiments  $S > 40$  is applied.

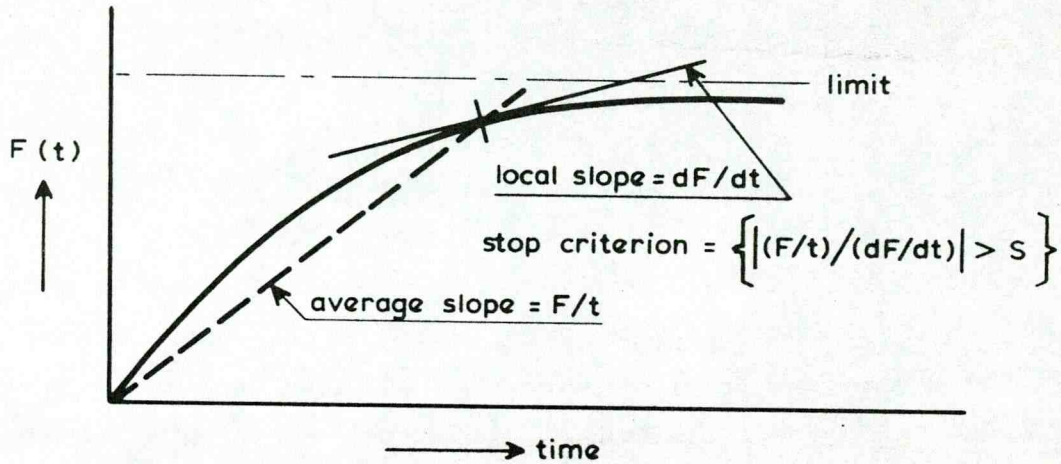


Figure 5. Definition of the Stop criterion, using a parameter  $S$ .

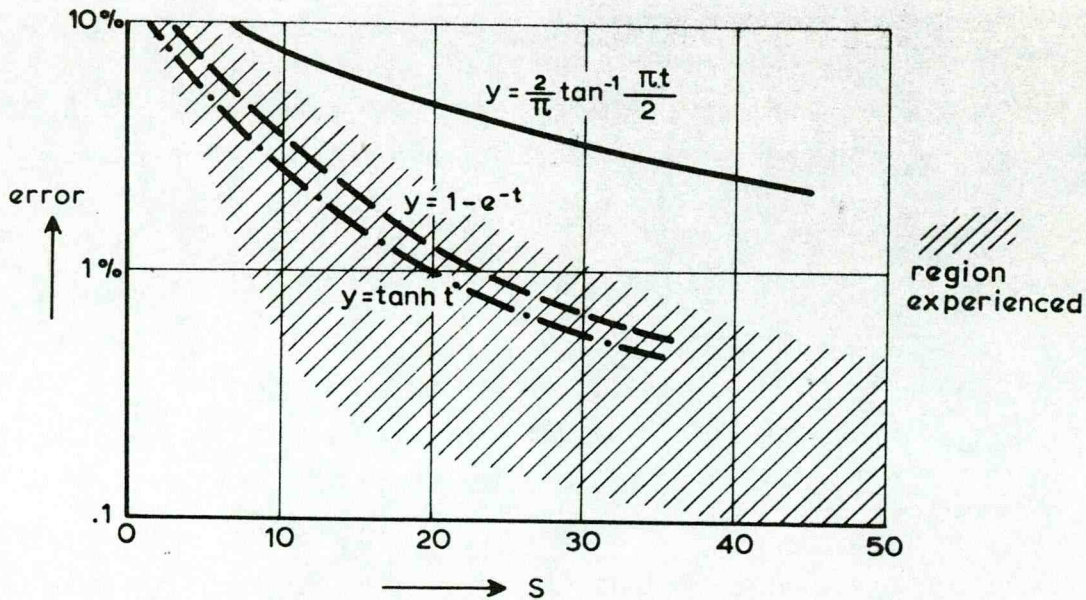


Figure 6. Stop experiences and theoretical values of the error for known asymptotic functions.

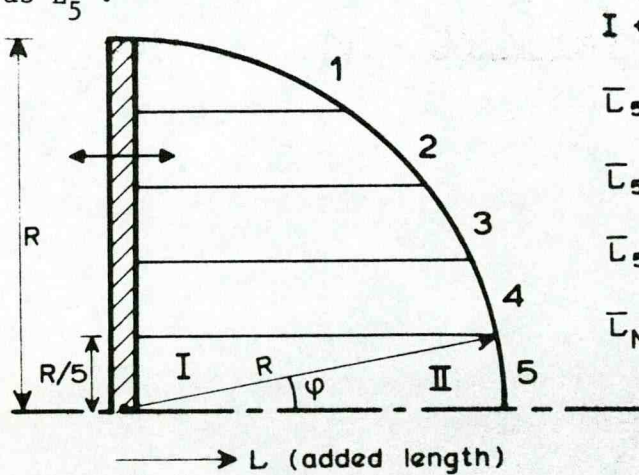


# 6. Accuracy check for computations of dams and for strips in infinite water

For a strip in infinite water, the analytical solution of Lamb [5] can directly be applied. The first accuracy check is for the total added mass per unit of length and the second for the maximum local pressure. For half the total added mass, situated at one side of the strip, we get

$$m_w = \frac{\pi}{4} \rho R^2 \quad (20)$$

in the following the added length  $L$  is used to represent the pressure distribution (pressure =  $\rho L \times$  acceleration). For a strip with width  $2a$  in infinite water, the radius of the circle encompassing the added water mass equals  $a$ , so  $R = a$ . In the example of Figure 7 we have divided the strip width in 5 elements (so  $N = 5$ ); the average added length of the lowest element we define as  $\bar{L}_5$ .



$$I + II = \bar{L}_5 R/5$$

$$\bar{L}_5 = (I + II) 5/R$$

$$\bar{L}_5/R = (1/2 R^2 \sin \varphi \cos \varphi + 1/2 R^2 \varphi) 5/R^2$$

$$\bar{L}_5/R = (5/2) (\sin \varphi \cos \varphi + \varphi)$$

$$\bar{L}_N/R = (n/2) (\sin \varphi \cos \varphi + \varphi)$$

$$\text{with } \varphi = \sin^{-1} (N^{-1})$$

Figure 7. Theoretical value of the average added length at the lowest strip element.

A second check is the  $L$  for the lowest element. In the theoretical solution the pressure distribution is represented by a quarter of a circle. The average pressure at the lowest element is, according to Figure 7, a little lower than radius  $R$ .

In the other case, that of a dam, the strip width ( $a$ ) is equal to the water depth and the solution found by Westergaard [8], but recalculated by Kolkman [3] is

$$L_{\max}/a = (8/\pi^2) \sum_{n=1}^{\infty} [\sin(n\pi/2)]/n^2 = 0.743 \quad (n \text{ is an odd integer}) \quad (21)$$

The height-average value appears to be

$$L_{av}/a = (16/\pi^3) \sum_{n=1}^{\infty} [\sin^2(n\pi/2)]/n^3 = 0.543 \quad (n \text{ is an odd integer}) \quad (22)$$

No correction factor is introduced for the finite height of the last element because there is no analytical solution available.

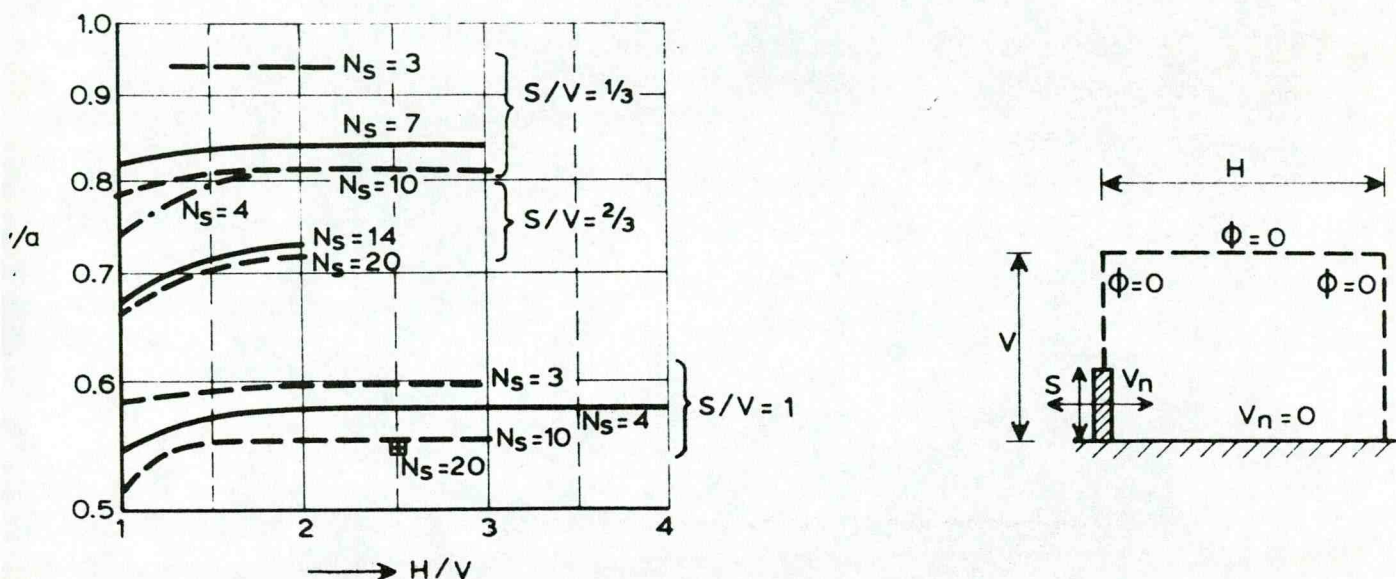


Figure 8. Effect of the grid width relative to the grid height.

A number of calculation results for horizontal water zones of varying width are summarized in Figure 8. The symbols used in this figure are  $V$  and  $H$  for the vertical and horizontal dimensions and  $S$  for the width of the strip which vibrates horizontally with a velocity  $V_n$ . It is obvious from the figure that a requirement for the infinite water condition is

$$H/V > 2, \quad (23)$$

The error for the smaller  $S/V$  ratios is not great even when  $H/V = 1$ .

Figure 9 shows that the water depth should be about 4 to 5 times the strip width to permit calculation of the infinite depth solution. The error due to a limited number of strip elements has then about reached its limit value.

An analysis of the influence of the limited number of strip elements ( $N$ ) on the results was made for the condition  $V/S = 4$ .

The pressures thus calculated were compared with the ones which could be analytically calculated.



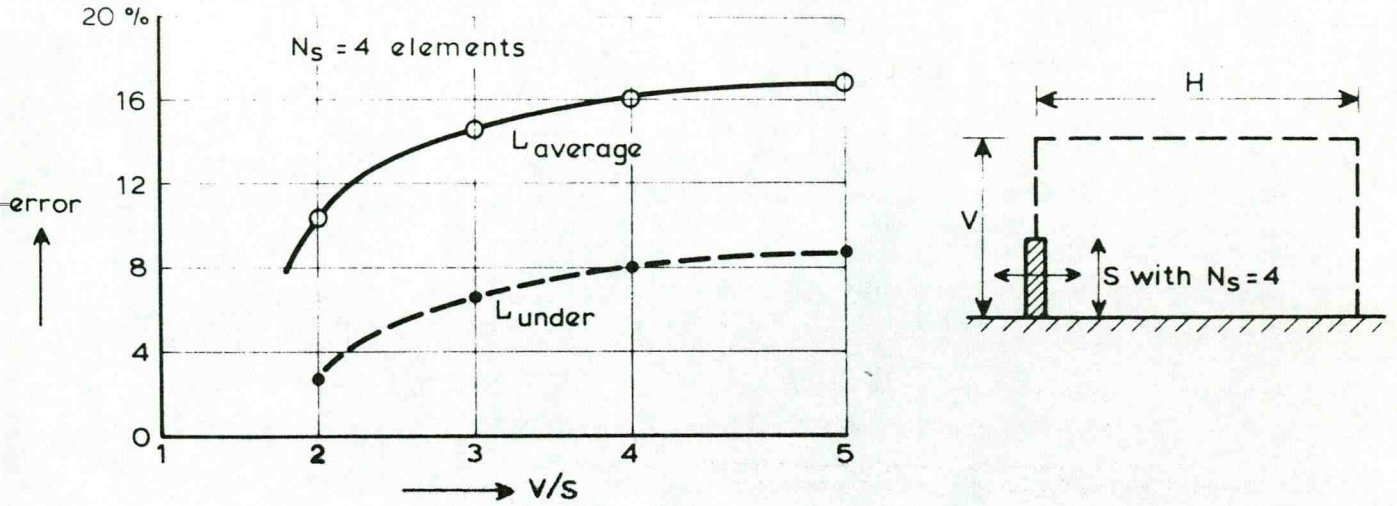


Figure 9. Effect of the water depth to strip width ratio on the error.

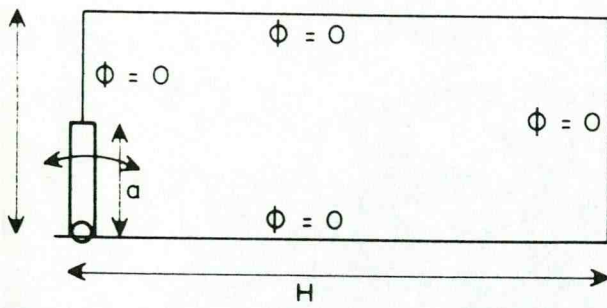
In numerical test runs it was found that the calculated added length appeared to be too great; the result was as if the strip was  $(0.3 \Delta L)$  too wide. For the average length this doubles the error; or better the calculated added mass per unit length is given by the equation

$$m_w = \rho \left( a + \frac{0.3 a}{N} \right)^2 \frac{\pi}{4} \quad (24)$$

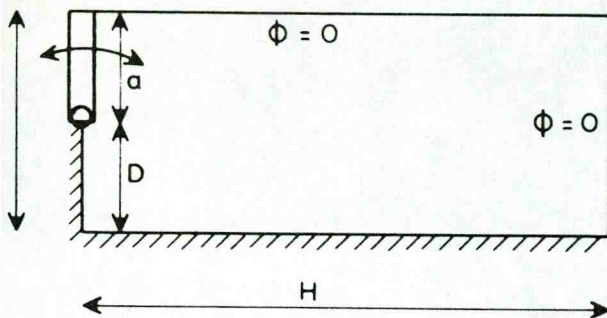
For instance, with 5 elements  $L_{\max}$  is 6% too large and  $L_{av}$  is 12% too large.

For a strip width equal to the water depth (the Westergaard problem of a dam at earthquake conditions), the error of the average added length appears from numerical experiments to be  $(N^{-2})$ . So, with a vision into 5 elements the error is 4%.

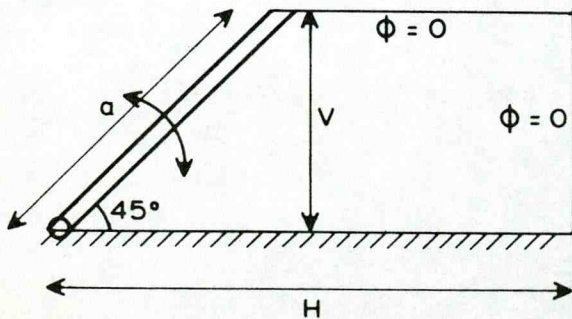
The much lower error with a "dam" is probably due to the absence of a sharp plate edge where the water has to pass at extremely high velocities. At edges with flow around them, the applied rectangular grid is in fact too coarse and this will hamper the flow. Tests made with a resistance correction at the last element show that results there can easily be influenced. Initially it had been the intention to give a recipe for this correction, but results proved not to be sufficiently consistent.



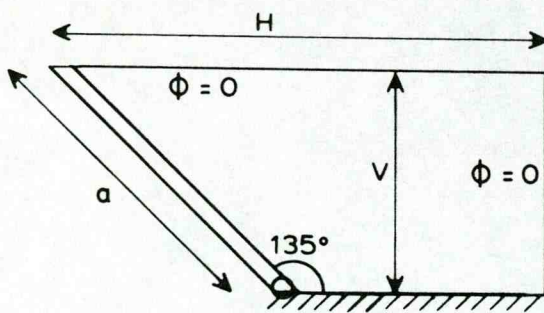
Rotating strip, height a					
$N_S$	6	6	6	8	10
$N_V$	30	20	10	30	25
$N_H$	60	40	20	60	40
$I_p / \rho a^4$	0,120	0,120	0,120	0,115	0,111



Rotating flap, height a				
$N_S$	10	10	10	10
$N_D$	0	2	2	5
$N_H$	30	25	40	40
$I_p / \rho a^4$	0,107	0,101	0,101	0,085



Rotating flap, length a		
$N_V$	10	15
$N_H$	40	50
$I_p / \rho a^4$	0,176	0,172



Rotating flap, length a			
$N_V$	5	10	15
$N_H$	20	40	60
$I_p / \rho a^4$	0,093	0,089	0,089

a = length of the flap gate

$N_H, N_V, N_S, N_D$  = number of elements.

$I_p$  = polar moment of inertia per unit of width

Figure 10 Computation results for various situations.



## 7. Computation results for various configurations

In Figure 10 the results of computed added mass for various rotating flap gates are presented but now this mass is expressed in terms of a polar moment of inertia. In the upper figure some computation results with a strip in ample water are presented with potential  $\phi = 0$  at the horizontal axis of symmetry. This results can be directly compared with the results found with Lamb's analytical solution [5] of a rotating strip with width  $2a$ .

$$I_p = \frac{\pi}{32} \rho a^4 = 0.098 \rho a^4 \quad (25)$$

It has been found that for rotating strips errors are greater than in the case of translating strips, probably because flow around the edge is relatively stronger at rotation.

Without further check it is assumed that the errors are much smaller for a rotating flap gate; because its cuts the waterlevel no flow goes around a edges.

## 8. Conclusions

The proposed procedure for the added mass calculation, using the spread sheet method, is easy and the desired versatility is achieved. The calculation time can be estimated and the Stop procedure is effective. With overrelaxation, used to shorten the calculation time, a check is needed on whether the solution is stable and reached without an overshoot. Accuracy tests are presented and they show that for an accuracy of the order of 10% and for relatively simple test configurations the required number of grid points remains reasonably small.



Symbols

$a$	strip width	(m)
$\bar{a}_s$	acceleration vector	(m s <sup>-2</sup> )
$I_p$	added polar moment of inertia	(kg m <sup>2</sup> )
$L$	added length	(m)
$m_w$	added mass	(kg)
$N_H$	number of grid points in horizontal sense	
$N_V$	number of grid points in vertical sense	
$N_S$	number of elements in vibrating strip	
$p$	pressure	(Pa)
$R$	overrelaxation factor (with $R > 1$ )	
$S$	parameter used in the stop criterion	
$t$	time	
$\bar{V}$	velocity (vector)	(m s <sup>-1</sup> )
$\bar{V}_n$	velocity component normal to boundary	(m s <sup>-1</sup> )
$\bar{V}_s$	vibration velocity of the structure	(m s <sup>-1</sup> )
$\bar{V}_{sn}$	velocity component normal to gate boundary	(m s <sup>-1</sup> )
$\bar{V}_h$	horizontal velocity component	(m s <sup>-1</sup> )
$\bar{V}_v$	vertical velocity component	(m s <sup>-1</sup> )
$x$	horizontal distance in metre or in number of points	
$y$	vertical distance in metre or in number of points	
$y$	vibrational displacement	(m)
$\Delta L$	mesh width	(m)
$\alpha$	gate angle	
$\Delta q$	discharge per element	(m <sup>2</sup> s <sup>-1</sup> )
$\Delta t$	computation time of a single calculation	(s)
$\Phi$ or $\Phi(x,y)$	potential	(m <sup>2</sup> s <sup>-1</sup> )
$\Delta\Phi$	potential step	(m <sup>2</sup> s <sup>-1</sup> )
$\rho$	fluid density	(kg m <sup>-3</sup> )
$\omega$	angular vibrational frequency	(rad s <sup>-1</sup> )

Indices L, R, H and D refer to left, right, up and down.

Index n refers to direction normal to boundary.

Index s refers to the boundary of the gate.

References

1. Ames, W.F., "Numerical Methods for Partial Differential Equations", Academic Press, NY, 2nd ed. 1977.
2. Jennings, A., "Added Mass Fluid-Structure Vibration Problems", Int. Journ. for Numerical Methods in Fluids, Vol. 5, pp. 817-830 (1985).
3. Kolkman, P.A., "Flow-Induced Gate Vibrations", Thesis Delft Techn. Univ.; publ. 164 Delft Hydr. Lab., 1976.
4. Kolkman, P.A., "Vibrations of Hydraulic Structures" in: "Developments in Hydraulic Engineering-2", editor P. Novak, publ. Elsevier Appl. Science Publishers 1984.
5. Lamb, H., "Hydrodynamics", 6th ed. Cambridge Univ. Press, 1932.
6. Olsthoorn, T.N., "Modelleren zonder speciale programma's",  $H_2O$ , Vol. 171 nr. 3., 1984.
7. Wendel, K., "Hydrodynamische Masse und hydrodynamische Massenträgheitsmomente", Jahrbuch der Schiffbautechnischen Gesellschaft, Vol. 44, 1950.
8. Westergaard, H.M., "Water Pressures on Dams during Earthquakes", Transact. A.S.C.E. 1933, paper 1835.



## Appendix

The set of potential equations to be used for the conditions of figure 4, where the inner elements are marked with (1), the upper left corner element with (2), etc.

The indices L, R, U, and D refer to "left", "right", "up" and "down", respectively

- 1) the inner elements (see Equation 12):

$$\phi = (\phi_L + \phi_U + \phi_R + \phi_D)/4$$

- 2) the left corner element at the top:  
two boundaries have  $\phi = 0$ , see equation 14.

$$\phi = (\phi_R + \phi_D)/6$$

- 3) the left elements above the gate:

$$\phi = (\phi_U + \phi_R + \phi_D)/5$$

- 4) the left elements at the gate (apart from the lowest one) where discharge  $\Delta q_L$  is introduced by the gate movement:

$$\phi = (\Delta q_L + \phi_U + \phi_R + \phi_D)/3$$

- 5) the left corner element, at the bottom, with  $\Delta q_L$  introduced by the gate and  $\Delta q_D = 0$ :

$$\phi = (\Delta q_L + \phi_U + \phi_R)/2$$

- 6) the elements at the bottom where  $\Delta q_D = 0$ :

$$\phi = (\phi_L + \phi_U + \phi_R)/3$$

7) the right corner element at the bottom:

$$\phi = (\phi_L + \phi_U)/4$$

8) the elements at the right, except the corner elements:

$$\phi = (\phi_L + \phi_U + \phi_D)/5$$

9) the upper right corner element:

$$\phi = (\phi_L + \phi_D)/6$$

10) the element at the water surface, except the corner elements:

$$\phi = (\phi_L + \phi_R + \phi_D)/5$$



Bijlage 2 Rekenprogramma en voorbeeld berekening waarbij een verticale klep  
op een vlakke bodem staat en een roterende trilling uitvoert

\$ DEBUG

C        Programmanaam : ADD-MASS.FOR

C        Datum         : 01-10-1987

C        Beschrijving : Berekening van toegevoegde watermassa  
C                        met behulp van potentiaal theorie in  
C                        combinatie met de relaxatie methode.

Algemene  
informatie  
programma

C        Variabelen    : OR = overrelaxatie  
C                        SH = schuifhoogte  
C                        WD = waterdiepte  
C                        HU = horizontale uitgestrektheid  
C                        ES = eindstop  
C                        SD = schuifdebiet  
C                        PT = potentiaal  
C                        OP = oude potentiaal  
C                        NP = nieuwe potentiaal  
C                        TD = tijd  
C                        DK = druk  
C                        MM = moment  
C                        VM = vorig moment  
C                        I = teller  
C                        X = nummer knooppunt X-richting  
C                        Y = nummer knooppunt Y-richting  
C                        WN = waar/niet-waar tuimelaar

C        Data

REAL    OR, TD, ES, MM, VM, ST, OP, NP  
INTEGER SH, WD, HU, I, X, Y  
LOGICAL WN

data declaratie  
(dimensie arrays  
afhankelijk van  
grootte rooster)

C        Arrays

REAL DK(30), PT(100,30), SD(30)

C        Beginwaarden invoeren

OR = 1.5  
SH = 6  
HU = 60  
WD = 30  
ES = 50.0

invoer via  
scherm

C        Schuifdebiet lineaire verdeling

DO 10 I = 1, SH, 1  
SD(I) = I - 0.5  
10       CONTINUE

debietverdeling  
voor rotatie van  
schuif  $q = y_s \cdot \Delta y \cdot \omega$

C        Beginwaarden

      I = 0  
      VM = 0

beginwaarden

C        Lus

20       I = I + 1

      DO 50 X = 1, HU, 1  
      DO 40 Y = 1, WD, 1

      OP = PT(X,Y)

      IF (X .EQ. 1 .AND. Y .EQ. 1) THEN  
      NP = (SD(1) + PT(2,1) + PT(1,2))/4  
      GOTO 30  
      ENDIF

      IF (X .EQ. 1 .AND. Y .EQ. WD) THEN  
      NP = (PT(X+1,Y) + PT(X,Y-1))/6  
      GOTO 30  
      ENDIF

      IF (X .EQ. HU .AND. Y .EQ. 1) THEN  
      NP = (PT(X-1,Y) + PT(X,Y+1))/6  
      GOTO 30  
      ENDIF

      IF (X .EQ. HU .AND. Y .EQ. WD) THEN  
      NP = (PT(X-1,Y) + PT(X,Y-1))/6  
      GOTO 30  
      ENDIF

      IF (X .EQ. 1 .AND. Y .LE. SH) THEN  
      NP = (PT(X,Y+1) + PT(X,Y-1) + PT(X+1,Y) + SD(Y))/3  
      GOTO 30  
      ENDIF

      IF (X .EQ. 1 .AND. Y .GT. SH) THEN  
      NP = (PT(X,Y+1) + PT(X,Y-1) + PT(X+1,Y))/5  
      GOTO 30  
      ENDIF

      IF (X .EQ. HU) THEN  
      NP = (PT(X-1,Y) + PT(X,Y+1) + PT(X,Y-1))/5  
      GOTO 30  
      ENDIF

      IF (Y .EQ. 1) THEN  
      NP = (PT(X-1,Y) + PT(X+1,Y) + PT(X,Y+1))/5  
      GOTO 30  
      ENDIF

toekennen waarde  
van potentiaal  
afhankelijk van  
ligging punt in  
geometrie



	IF (Y .EQ. WD) THEN	
	NP = (PT(X-1,Y) + PT(X+1,Y) + PT(X,Y-1))/5	
	GOTO 30	
	ENDIF	
	NP = (PT(X-1,Y) + PT(X+1,Y) + PT(X,Y-1) + PT(X,Y+1))/4	
30	PT(X,Y) = OP + (NP - OP)*OR	
40	CONTINUE	
50	CONTINUE	
	MM = 0	
	DO 60 J = 1, SH, 1	
	DK(J) = PT(1,J) + (0.5 * SD(J))	
	MM = MM + ((J - 0.5) * DK(J))	berekening druk en moment
60	CONTINUE	
	WRITE (*,130) MM	
	WN = 'FALSE'	
	IF (VM .NE. MM) THEN	
	ST = ABS((MM/I)/(MM-VM))	
	ELSE	
	ST = 1000	
	ENDIF	uitvoer rekenlagen
	WRITE (*,140) ST	
	WRITE (*,150) I	
	WRITE (*,160)	
	VM = MM	
	IF (ST .LE. ES) THEN	
	GOTO 20	
	ENDIF	stopcriterium
C	Uitvoeren resultaten	
	WRITE (*,180)	
	WRITE (*,130) MM	
	WRITE (*,150) I	
	WRITE (*,140) ST	
	WRITE (*,*) ' '	uitvoer resultaten
	DO 70 J = 1, SH, 1	
	WRITE (*,170) J, DK(J)	
70	CONTINUE	

C       Formatering

```
80       FORMAT (' Factor over-relaxatie [1.5]       : ' )
90       FORMAT (' Aantal roosterpunten schuif       : ' )
100       FORMAT (' Aantal roosterpunten in X-richting: ' )
110       FORMAT (' Aantal roosterpunten in Y-richting: ' )
120       FORMAT (' Grootte stopcriterium iteratie   : ' )
130       FORMAT (' Moment                       = ' F10.3)
140       FORMAT (' Stopparameter               = ',F10.3)
150       FORMAT (' Aantal iteraties = ',I6)
160       FORMAT (' -----')
170       FORMAT (' Wandpotentiaal element ',I3,' = ',F10.3)
180       FORMAT (/' RESULTATEN '/' -----'/)
C       Einde
```

END

formatering



```

C:/FOR>Add-mass
Factor over-relaxatie [1.5]      : 1.5
Aantal roosterpunten schuif      : 6
Aantal roosterpunten in x-richting : 60
Aantal roosterpunten in y-richting : 30
Grootte stopcriterium iteratie   : 50.0

```

opdracht programma

invoer programma  
via scherm

```

Moment      = 91.151
Stopparameter = 1.000
Aantal iteraties = 1

```

```

Moment      = 115.271
Stopparameter = 2.390
Aantal iteraties = 2

```

```

Moment      = 128.894
Stopparameter = 3.154
Aantal iteraties = 3

```

```

Moment      = 137.480
Stopparameter = 4.003
Aantal iteraties = 4

```

```

Moment      = 143.063
Stopparameter = 5.125
Aantal iteraties = 5

```

```

Moment      = 146.724
Stopparameter = 6.679
Aantal iteraties = 6

```

```

Moment      = 149.120
Stopparameter = 8.890
Aantal iteraties = 7

```

```

Moment      = 150.753
Stopparameter = 11.545
Aantal iteraties = 8

```

```

Moment      = 151.953
Stopparameter = 14.063
Aantal iteraties = 9

```

```

Moment      = 152.876
Stopparameter = 16.562
Aantal iteraties = 10

```

```

Moment      = 153.592
Stopparameter = 19.500
Aantal iteraties = 11

```

```

Moment      = 154.156
Stopparameter = 22.780
Aantal iteraties = 12

```

rekenslagen  
programma op  
scherm

Moment	=	154.608
Stopparameter	=	26.340
Aantal iteraties	=	13

Moment	=	154.974
Stopparameter	=	30.229
Aantal iteraties	=	14

Moment	=	155.274
Stopparameter	=	34.437
Aantal iteraties	=	15

Moment	=	155.524
Stopparameter	=	38.986
Aantal iteraties	=	16

Moment	=	155.732
Stopparameter	=	43.883
Aantal iteraties	=	17

Moment	=	155.909
Stopparameter	=	49.126
Aantal iteraties	=	18

Moment	=	156.059
Stopparameter	=	54.726
Aantal iteraties	=	19

### RESULTATEN

Moment	=	156.059
Aantal iteraties	=	19
Stopparameter	=	54.726

Wandpotentiaal element	1 =	1.575
Wandpotentiaal element	2 =	4.613
Wandpotentiaal element	3 =	7.290
Wandpotentiaal element	4 =	9.306
Wandpotentiaal element	5 =	10.234
Wandpotentiaal element	6 =	9.364

rekenslagen  
programma op  
scherm  
(vervolg)

uitvoer  
programma op  
scherm

Roterende verticale klep die op de bodem staat in ruimwater.

De debieten worden ingevoerd volgens  $\omega = 1$ , elementgrootte 1, dus  $q = z\omega$

$$\frac{M_w}{\rho h^4_{\text{schuif}}} = \frac{\text{"Moment"}}{(\text{aantal schuifelementen})^4} = \frac{156,059}{64} = 0.1204$$





p.o. box 177

2600 mh delft

the netherlands